

# PROGRESSIVE DENOISING MODEL FOR FINE-GRAINED TEXT-TO-IMAGE GENERATION

Zhengcong Fei, Mingyuan Fan, Junshi Huang\*, Xiaoming Wei, Xiaolin Wei

Meituan

Beijing, China

{name}@meituan.com

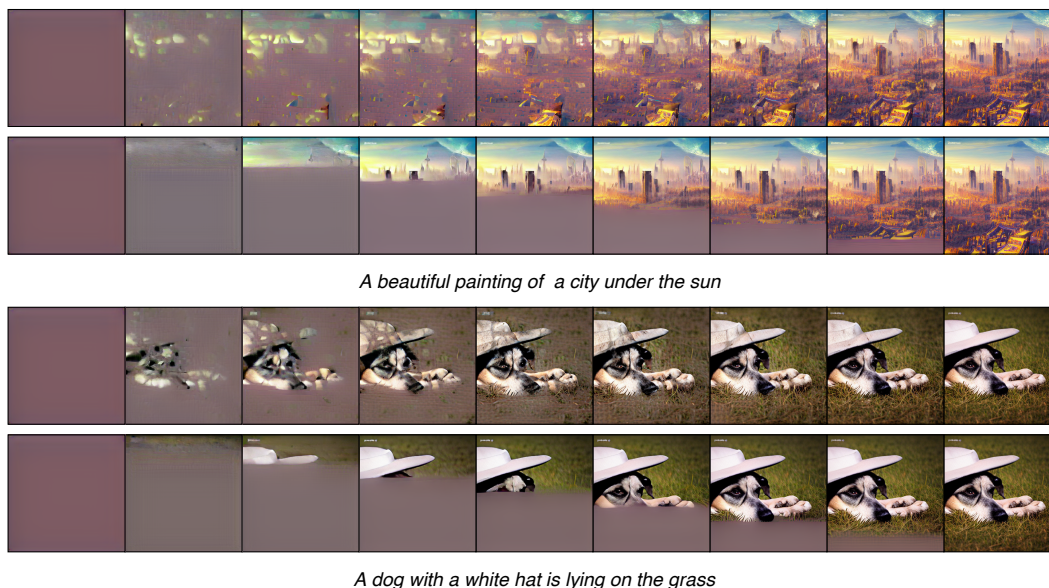


Figure 1: Illustration of different generation orders for text-to-image synthesis.

## ABSTRACT

Recently, vector quantized autoregressive (VQ-AR) models have shown remarkable results in text-to-image synthesis by equally predicting discrete image tokens from the top left to bottom right in the latent space. Although the simple generative process surprisingly works well, is this the best way to generate the image? For instance, human creation is more inclined to the outline-to-fine of an image, while VQ-AR models themselves do not consider any relative importance of each component. In this paper, we present a progressive denoising model for high-fidelity text-to-image image generation. The proposed method takes effect by creating new image tokens from coarse to fine based on the existing context in a parallel manner and this procedure is recursively applied until an image sequence is completed. The resulting coarse-to-fine hierarchy makes the image generation process intuitive and interpretable. Extensive experiments demonstrate that the progressive model produces significantly better results when compared with the previous VQ-AR method in FID score across a wide variety of categories and aspects. Moreover, the text-to-image generation time of traditional AR increases linearly with the output image resolution and hence is quite time-consuming even for normal-size images. In contrast, our approach allows achieving a better trade-off between generation quality and speed.

\*Corresponding author.

---

## 1 INTRODUCTION

The task of text-to-image generation aims to create natural and consistent images from the input text and has received extensive research interest. Recently, latent autoregressive (AR) generation frameworks have achieved great success in advancing the start-of-the-arts, by learning knowledge and patterns from a large-scale multimodal corpus (Radford et al., 2021; Li et al., 2021; Yu et al., 2022a). Generally, they treat the task as a form of language modeling and use Transformer-like (Vaswani et al., 2017) architectures to learn the relationship between language inputs and visual outputs. A key component of these approaches is the conversion of each image into a sequence of discrete units through the use of a VQ-VAE (Van Den Oord et al., 2017) based image tokenizer, e.g., VQ-GAN (Esser et al., 2021b; Yu et al., 2021), RQ-VAE (Lee et al., 2022a) and ViT VQ-GAN (Yu et al., 2021). Visual tokenization essentially unifies the view of text and images so that both can be treated simply as sequences of discrete tokens and is adaptable to sequence-to-sequence models. To that end, DALL-E (Ramesh et al., 2021), CogView (Ding et al., 2021), RQ-Transformer (Lee et al., 2022a), and Parti (Yu et al., 2022b) employed autoregressive (AR) language models, to learn from a large collection of potentially noisy text-image pairs (Changpinyo et al., 2021; Jia et al., 2021; Gafni et al., 2022). In particular, Wu et al. (2022) further expands on this AR over AR modeling approach to support both arbitrarily-sized image generation.

Another research line for text-to-image generation involves diffusion-based methods, such as GLIDE (Nichol et al., 2021), DALL-E 2 (Ramesh et al., 2022), stable diffusion (Rombach et al., 2022), RQ-Transformer (Lee et al., 2022a), and Imagen (Saharia et al., 2022). These models pursue to directly generate images or latent image features with diffusion process (Ho et al., 2020; Dhariwal & Nichol, 2021) and produce images with markedly high-quality and great aesthetic appeal. Even so, discrete sequence modeling for text-to-image generation remains appealing given extensive prior work on large language models (Brown et al., 2020) and advances in discretizing other modalities, such as video and audio, as cross-language tokens (Bond-Taylor et al., 2021). However, the current constructed plain and equal paradigm, without enough global information (Tan et al., 2021), may not reflect the progressive hierarchy/granularity from high-level concepts to low-level visual details and is not in line with the actual human image creation. Also, the time complexity of standard auto-regressive image sequence generation is  $\mathcal{O}(n)$ , which meet limitations for high resolution.

Motivated by the above, we present the *progressive denoising model* for text-to-image generation from coarse to fine. Specifically, it takes text tokens as inputs to an encoder and progressively predicts discrete image tokens with a decoder in the latent space. The image tokens are transformed by the VQ-GAN, which can produce high-quality reconstructed outputs. As illustrated in Figure 1, given text prompts, our model first generates high-level content skeleton, then these information are used as pivoting points at which to create details of finer granularity. This process iterates until an image is finally completed by adding the fine-grained tokens. We show that such progressive generation in a latent space is an effective way to improve text-to-image performance, enabling to accurately integrate and visually convey world knowledge.

To assess the performance, we conduct text-to-image generation experiments on the popular MS COCO (Lin et al., 2014) benchmark. Compared with the convention AR model with similar model parameters, our method achieves significantly better image generation performance, as measured by image quality and image-text alignment in both automatic metrics and human evaluations. The progressive model also provides important benefits for the inference speed with learned error recovering. As the inference time of AR methods increases linearly with the output image resolution, the progressive model provides the global context for image token prediction and employs the importance score for parallel set selection. This allows us to provide an effective way to achieve a better trade-off between the inference speed and the image quality. We hope this technique can help visual content creators to save time, cut costs and improve their productivity and creativity.

Finally, we summarize our contributions as follows: *i) Order matters.* We argue that the importance of image tokens is not equal and present a novel progressive denoising model in the VQ-based latent space for text-image generation. Compared with previous work, our method allows long-term control over a generation due to the top-down progressive structure and enjoys a significant reduction over empirical time complexity. *ii)* We use large-scale pre-training and *learned error recovering* mechanism customized to our approach, to further boost image generation performance. *iii)* Experiments on the dataset across different aspects demonstrate the superiority of progressive

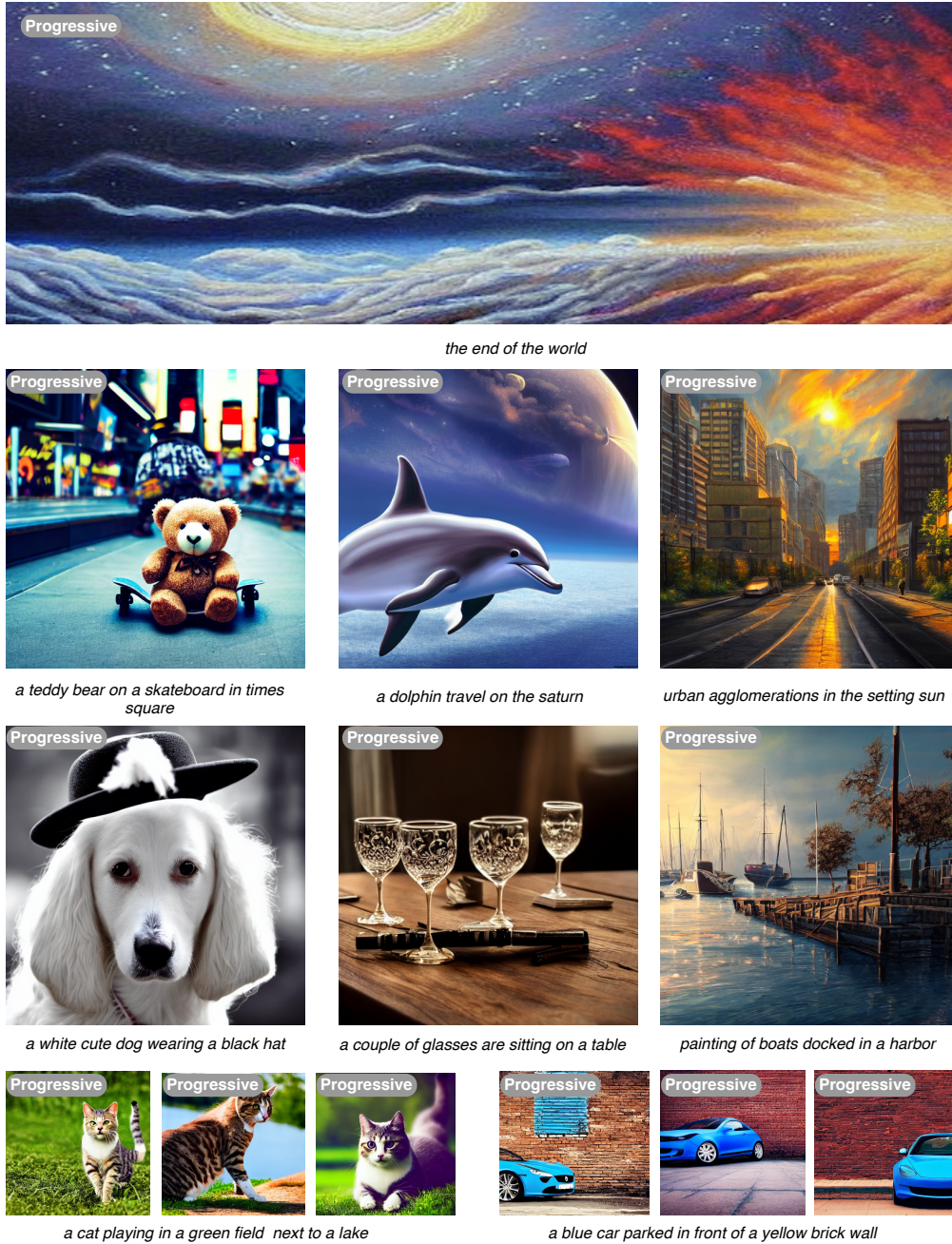


Figure 2: Generated images and corresponding text prompts from the progressive denoising model. Refer to Section 4.3 for a more detailed discussion.

model over strong baselines. In particular, our approach is simple to understand and implement, yet powerful, and can be leveraged as a building block for future text-to-image synthesis research.

## 2 BACKGROUND

We first briefly introduce the learning discrete latent space of images via VQ-VAE and leverage a transformer to learn the mapping from text to image. Specifically, the two-stage text-to-image process includes 1) training an image tokenizer that turns an image into a sequence of discrete visual

tokens for training and reconstructing an image at inference time and 2) optimizing a sequence-to-sequence Transformer model that produces image tokens from text tokens.

**Image Tokenizer.** Since the computation cost is quadratic to the sequence length and low-level semantic representations, it is limited to directly modeling raw pixels using transformers (Chen et al., 2020). Previous works (Van Den Oord et al., 2017; Yu et al., 2021) addressed this by using a discrete variational auto-encoder (VAE), where a visual codebook is learned that maps a patch embedding to its nearest codebook entry in the latent space. These entries can be thought of as visual words, and the appearance of these words in a patch in a given image is thus contained image tokens like words in a sentence. A VQ-VAE image tokenizer usually follows an encoder-decoder paradigm and is trained with the losses as (Esser et al., 2021b) on the unlabeled images of training data. Specifically, the encoder  $E$ , the decoder  $D$  and the codebook  $Z \in \{z_k\}_{k=1}^K$ , where  $K$  is the code size, can be trained end-to-end via the following loss with input image  $Y$ :

$$L_{vae} = \|Y - \tilde{Y}\|_1 + \|\text{sg}[E(Y) - z_q]\|_2^2 + \beta \|\text{sg}[z_q] - E(Y)\|_2^2, \quad (1)$$

$$z_q = Q(z) = \arg \min_{z_k \in Z} \|z - z_k\|_2^2, \quad (2)$$

where  $\tilde{Y}$  is reconstructed image from  $D(z_q)$  and  $z_q$  is the indexed discrete code.  $z = E(Y)$  and  $Q(\cdot)$  is mapping function from spacial feature  $z$  to  $z_q$ .  $\text{sg}[\cdot]$  stands for the stop-gradient operation. In practice, we use VQ-GAN (Esser et al., 2021b) with techniques including factorized codes and real-false discriminator for perception loss and exponential moving averages (EMA) to update the codebook entries which contribute to training stability and reconstruction quality.

**Text-to-Image Transformer.** After unified image and text modalities with discrete tokens, a standard encoder-decoder Transformer model is then trained by treating text-to-image generation as a sequence-to-sequence modeling problem. The Transformer model takes text prompt as input and is trained using next-token prediction of image latent codes supervised from the image tokenizer. Formally, provided with text prompt  $X$ , the optimization objective for modeling of image token sequence  $Y = \{y_1, \dots, y_L\}$  in training dataset  $\mathcal{D}$  can be factorized as:

$$L_{ar} = -\log p(Y|X) = -\log \prod_{i=1}^L p(y_i | y_{<i}, X). \quad (3)$$

During inference, the model samples image tokens autoregressively conditioned on context, which are later decoded into pixels using the VQ-GAN decoder to create the output image. For the text encoder, we load a pre-trained BERT-like model (Kenton & Toutanova (2019); Raffel et al. (2020)) for training acceleration, and the decoding part of image tokens is trained from random initialization. Most of the existing latent-based text-to-image generation models can be split as decoder-only (Ramesh et al., 2021; Ding et al., 2021), encoder-decoder (Yu et al., 2022b) and diffusion models (Rombach et al., 2022) in the VQ-VAE based latent space. In this paper, we chose to focus on the encoder-decoder pattern with trained text encoding.

### 3 METHODOLOGY

#### 3.1 OVERVIEW

Provided with a text prompt  $X$ , we aim to generate a complete image sequence  $Y$ , where the reconstructed image from VQ-GAN is accordingly semantic correct and high fidelity. The generation procedure of our method can be formulated as a progressive sequence of  $T$  stages:  $Y = \{Y^1, \dots, Y^T\}$ , such that for  $t$ -th stage,  $Y^t$  is an advanced sequence of  $Y^{t-1}$ . The following stage can be perceived as a finer-resolution image sequence compared to the preceding stage. In between, intermediate sequence is formed as  $Y^t = \{y_1^t, \dots, y_L^t\}$  and the corresponding state sequence  $Z^t = \{z_1^t, \dots, z_L^t\}$ , where  $\mathcal{V}$  is a VQ code vocabulary, and  $L$  is the image sequence length.  $y_i^t \in \mathcal{V}$  and  $z_i^t \in \{0, 1, -1\}$ . The state sequence 0, 1, -1 indicate that the current position of the intermediate sequence is unchanged, to be generated, or to be replaced. Hence, the consecutive pairs are related to each other by  $y_i^{t+1} = (1 - |z_i^{t+1}|)y_i^t + z_i^t \tilde{y}_i^{t+1}$ , where  $\tilde{y}_i^{t+1} \in \mathcal{V}$  is a newly predicted image token for the position  $i$ . Note that the constraint in each stage includes:  $\forall t, \sum_i^L \mathbb{I}[z_i^t = 1] = \frac{L}{T}$ , and



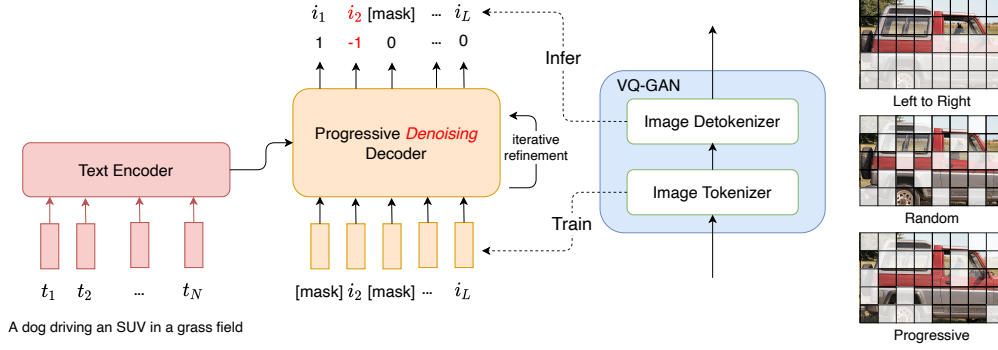


Figure 3: Overview of the proposed progressive text-to-image model with left-to-right, random, and coarse-to-fine generation orders in the VQ-GAN latent space.

$\sum_i^L \mathbb{I}[z_i^t = -1] \leq \sum_i^L \mathbb{I}[z_i^{t-1} = 1]$ . Finally, the generation procedure with  $T$  stages can be modeled with factorized conditional probability as:

$$p(Y|X) = \prod_{t=1}^T \prod_{i=1}^L p(y_i^{t+1} | Y^{\leq t}, X, z_i^{t+1}) p(z_i^{t+1} | Y^{\leq t}, X). \quad (4)$$

At each generation step  $t$ , model first produces the position state sequence  $Z^{t+1}$  for the updated position according to  $p(z_i^{t+1} | Y^{\leq t}, X)$ . Once the changeable image token set is determined, the corresponding token is generated according to distribution  $p(y_i^{t+1} | Y^{\leq t}, Z^{t+1}, X)$ , leading to a new image sequence  $Y^{t+1}$ . Thus, we can recover the final image token sequence  $P(Y|X)$  by marginalizing all the intermediate sequences. Note that such pair generation procedure starts from a fully masked image sequence  $\{[mask], \dots, [mask]\}$  of length  $L$ , iteratively fills and recovers image tokens, and terminates after  $T$  steps with image sequence  $Y^T$  in the latent space.

### 3.2 IMAGE TOKEN SET SELECTION

Two properties are desired for a progressive generation: *i*) important and easy tokens should appear in an earlier stage, so that the generation follows a coarse-to-fine manner; *ii*) the number of stages should be small, thus the generation maintains fast at inference time. In between, the key points of the progressive model lie the importance score to define the generation order at each stage, as shown in Figure 3. In the following paragraphs, we introduce two variants for image token set scoring instead of random selection.

**Constant Quantization Error Scoring.** As the quantization error of VQ-GAN reflects the difficulty of the image patch to discretize or represent the patch, we can decide the token order on the intermediate sequences through the error size, also referred to as the confidence of image tokenizer. Specifically, we can then train a confidence-aware Transformer model based on the ranked confidence score  $c(\cdot)$  of ground-truth image sequences from the image tokenizer as:

$$p(z_i^{t+1} = 1 | Y^{\leq t}, Z^t, X) \sim \text{Softmax}(c(y^T)). \quad (5)$$

Then, at each time  $t$ , the top- $K$  high-confidence image token is used to predict while masking the residual, where  $K = \frac{L}{T}$ . Intuitively, we prefer to generate a token in the later stage if it is full of uncertainty, i.e., more global context is needed to determine it. The training pairs reverse the generation process, and each training instance  $(X, Y)$  is broken into a consecutive series of tuples  $(X, Y^0, Z^1, Y^1), \dots, (X, Y^{T-1}, Z^T, Y^T)$  with pre-calculated error scoring.

**Dynamic Importance Scoring.** We further propose to learn an image token set selection distribution that selects position in order to maximize a reward function that we specify. In this case, we refer to the position selection distribution as a policy  $\pi_\theta(a_t | s_t)$ , where a state  $s_t$  is  $(Y^{\leq t}, Z^t, X)$ , an action  $a_t \in \{1, \dots, L\}$  is an updating sequence, so that  $Z^{t+1}$  is 1 or  $-1$  at position  $a_t$  and 0 elsewhere, and  $\pi_\theta$  is parameterized using a neural network. Beginning at a state  $s_1$  corresponding to an

input  $X$  with a fully masked sequence, we obtain a generation by repeatedly sampling an updating  $a_t \sim \pi_\theta(s_t)$  and transitioning to a new state for  $T$  steps. Each transition  $s_t$  consists of selecting an image token set. Given a scalar reward function  $r$ , *e.g.*, L2 loss for reconstructed image pixels (Dong et al., 2021) or CLIP embedding similarity (Radford et al., 2021), the objective is to find an optimal position policy that maximizes expected reward as,

$$L_{dis} = -E_{\tau \sim \pi_\theta(\tau)} \left[ \sum_{t=1}^T r(s_t, a_t) \right], \quad (6)$$

$$\pi_\theta(\tau) = p(s_1) \prod_{t=1}^T \pi_\theta(a_t | s_t) p(s_{t+1} | a_t, s_t), \quad (7)$$

where  $\tau = (s_1, a_1, \dots, s_T, a_T)$ . We maximize this objective by estimating its gradient using the policy gradient (Sutton et al., 1999) strategy.

### 3.3 ERROR RECOVERING

Although the preceding progressive training based on importance score makes the model capable of efficiently generating image sequences from coarse to fine, however, the model still can not recover from errors where image token errors have already occurred. Specifically, for the progressive paradigm, all new image tokens are simultaneously generated based on the existing context at the previous stage. Such an approach suffers from a conditional independence problem like non-autoregressive generation (Gu et al., 2018; Gu & Kong, 2021), in which the predicted tokens are conditional-independently generated and are agnostic of each other. Resultingly, it is prone to generating repeating or inconsistent new tokens at each generation round.

To alleviate this problem, we propose to train the progressive model to learn to recover from error generation, by *injecting pseudo error tokens* into the training data. Formally, at the  $t$ -th stage, given the tuple  $(X, Y^{t-1}, Y^t, Z^t)$ , we first randomly select part of generated image tokens from the  $Y^{t-1}$  and replaced them with other image tokens, except for  $[mask]$  token. Then, the corresponding position of sequence  $Z^t$  is instead with -1 to be labeled as updating. Finally, the new tuple is built for training data  $\mathcal{D}$ . However, injecting such pseudo error tokens to all training instances will mislead the model that generating then updating an error image token is a must-to-have behavior, which is not desired. Therefore, we inject pseudo error tokens into a training instance following  $\sim \text{Bernoulli}(p_{error})$  in this work. Besides, it would be better to recover the high-probability predicted by model while error image tokens, which we leave for future work.

## 4 EXPERIMENTS

This section presents experiments using the progressive model as introduced in section 3. We compare with state-of-the-art in section 4.1, analyze different generation order strategies and iterative step numbers in section 4.2, and present text-to-image cases in section 4.3.

The architecture of our progressive model closely follows VQ-GAN and standard encoder-decoder Transformer paradigm (Yu et al., 2022b). The only changes are the removal of the causal mask in the image decoder and the addition of state sequence prediction layer, with the order-aware training process. We use MS COCO (Lin et al., 2014) datasets identical to DALL-Eval (Cho et al., 2022) for evaluation in all experiments. For more implementation details please refer to the appendix.

Following prior works (Yu et al., 2022b; Cho et al., 2022), we evaluate the text-to-image generation performance using two primary axes: generated image quality, and alignment of the generated image with the input text. Specifically, the evaluation procedures include:

- **Image Quality.** Fréchet Inception Distance (FID) (Heusel et al., 2017) is used as the primary automated metric for measuring image quality. Specifically, the FID score is computed by inputting generated and real images into the Inception v3 (Szegedy et al., 2016) model, and using the output of the last pooling layer as extracting features. The features of the generated and real images are then used to fit two separate multi-variate Gaussians, respectively. Finally, the FID score is computed by measuring the Fréchet distance between the two multivariate Gaussian distributions.

Approach	Model Type	# Data	# Param	MS COCO FID ( $\downarrow$ )	
				Zero-shot	Fine-tuned
Retrieval Baseline	-	-	-	19.12	-
X-LXMERT	Autoregressive	180K	228M	37.4	-
DALL-E small	Autoregressive	15M	120M	45.8	-
minDALL-E	Autoregressive	15M	1.3B	24.6	-
CogView	Autoregressive	30M	4B	27.1	-
CogView2	Autoregressive	30M	9B	24.0	17.7
RQ-Transformer	Autoregressive	30M	3.9B	16.9	-
DALL-E 2	Diffusion	650M	5.5B	10.39	-
Imagen	Diffusion	860M	7.6B	7.27	-
Parti	Autoregressive	800M	20B	7.23	3.22
PDM	Progressive	20M	1.2B	13.28	5.34

Table 1: FID score comparison of different text-to-image synthesis models on the MS COCO dataset. Some listed evaluation results are from DALL-Eval and corresponding papers.

Approach	BLEU ( $\uparrow$ )	METEOR ( $\uparrow$ )	CIDEr ( $\uparrow$ )	SPICE ( $\uparrow$ )
Ground Truth (upper bound)	32.5	27.5	108.3	20.4
Retrieval Baseline	22.4	21.7	81.5	15.3
ruDALL-E-XL	13.9	16.0	38.7	8.7
minDALL-E	16.6	17.6	48.0	10.5
PDM	20.5	19.7	74.8	13.5

Table 2: Comparison for image captioning evaluation on the MS COCO test set.

- **Image-Text Alignment.** Text-image fit degree is estimated by automated captioning evaluation: an image output by the model is captioned with a trained Transformer-based model (Cornia et al., 2020) and then the similarity of the input prompt and the generated caption is assessed via conventional metrics BLEU (Papineni et al., 2002), CIDEr (Vedantam et al., 2015), METEOR (Denkowski & Lavie, 2014), and SPICE (Anderson et al., 2016).

#### 4.1 COMPARISON WITH THE STATE-OF-THE-ART METHODS

In this part, the text-to-image generation performance is estimated from two perspectives. Besides, we also use a retrieval baseline, *i.e.*, given a text prompt, we retrieve the most matched image in the *training set*, measured by the cosine similarity between the text embedding and the image embedding from the trained CLIP model (Radford et al., 2021). This can be done efficiently by using fast similarity search libraries FAISS (Johnson et al., 2019).

**Image Quality Evaluation.** Following prior works (Ramesh et al., 2021; Yu et al., 2022b), we use 30,000 generated and real image samples for evaluation from MS COCO 2014 dataset using the same input preprocessing with  $256 \times 256$  image resolution. We qualitatively compare the proposed method with several state-of-the-art methods, including autoregressive-based models X-LXMERT Cho et al. (2020), minDALL-E (Ramesh et al., 2021), CogView (Ding et al., 2021), CogView 2 (Ding et al., 2022), RQ-Transformer (Lee et al., 2022a), Parti (Yu et al., 2022b), and diffusion-based models, DALL-E 2 (Ramesh et al., 2022) and Imagen (Saharia et al., 2022). The evaluation results coupled with the size of training data and model parameters are illustrated in Table 1. We can observe that our progressive model, which has a similar parameter size to previous autoregressive-based models, has strong competitive performance while posing an advance in inference speeding. In particular, the progressive model shows strong generalization without fine-tuning on specific domains compared with miniDALL-E. Except for scaling more parameters, generation pattern exploration also holds promise for text-to-image creation.

**Image-text Alignment Evaluation.** The image captioning evaluation complements the FID score evaluation as an automatic image-text alignment measurement for text-to-image generation models.

Order	FID ( $\downarrow$ )	CIDEr ( $\uparrow$ )
Left to right	19.23	54.3
Random	20.15	51.2
Un-progressive	22.23	49.5
Const. Error	16.17	64.3
Progressive	13.28	74.8

Table 3: Effect of different generation orders.

# Iterative	FID ( $\downarrow$ )	CIDEr ( $\uparrow$ )	SpeedUp
8	19.80	53.5	97.1 $\times$
16	15.86	65.1	52.5 $\times$
64	13.28	74.8	13.2 $\times$
256	12.73	78.5	3.3 $\times$
1024	12.51	79.8	1 $\times$

Table 4: Effect of iterative steps.

Table 2 provides results of different models on the image captioning evaluation as an automatic image-text alignment measure. As we expected, the progressive model outperforms other popular autoregressive-based models on this measure, and it effectively closes the gap to the scores obtained for captions generated from the ground truth images. However, we also should care that these results are limited by the used image captioning model’s (Cornia et al., 2020) ability to discriminate between outputs from different approaches.

#### 4.2 MODEL ANALYSIS

**Whether the Generation Order Has Significant Impact?** To deeply analyze the effectiveness of generation order in text-to-image generation, we compare four different generation strategies under the same network architectures. All baselines predict 16 image tokens at each step except for left-to-right manner in 1 image token. As shown in Table 3, we notice that the synthesis performance drops when replacing the progressive with the random or conventional sequential, indicating that predicting words from easy to hard in an image sequence benefits the quality. As we expected, dynamic learning-based order shows more advance with constant error scoring. When training the model with anti-progressive order, *i.e.*, training examples to the decoder model in a fine-to-coarse manner, we can observe a significant performance decrease, affirming the value of coarse-to-fine progressive generation manner again.

**How Many Progressive Steps Should Take?** One of the motivations of this work is that at each stage the generation can be parallel, leading to a significant reduction in training and inference. As there exists a hyper-parameter iterative step in the progressive generation process, we answer the question by fixing the selected token number in each step. The acceleration evaluation is based on a single Nvidia V100 GPU in the MS COCO dataset. As shown in Table 4, we can find that when the iterative steps increase from 8 to 64, the result improves prominently, when it further increases to 256, it seems saturated with little improvements. So we set the default iterative steps number to 64 in our experiments. We believe that different from diffusion with noisy, the progressive process forward with clear and finite image tokens, which leads to a significant reduction in times.

**Effect of Error Recovering.** We also investigate the influence of error recovering in Section 3.3 and the results for zero-shot MS COCO are shown in Table 5, where  $p_{error}$  is the probability of injecting pseudo incorrect image tokens to each training tuples. From the estimation results, we can observe that: 1) Without using the error recovering, *i.e.*,  $p_{error} = 0$ , the FID score drops significantly, indicating that the error recovering mechanism is effective for performance improvements. 2) As  $p_{error}$  grows larger, the performance becomes increasing first and then drops, as we believe that too many pseudo errors make it hard to learn the implicit text-to-image mapping. 3) The model achieves best performance with  $p_{error} = 0.3$ , which will be defaulting setting in other experiments.

$p_{error}$	FID ( $\downarrow$ )
0.0	15.86
0.3	13.28
0.5	13.61
0.7	14.90
1.0	16.65

Table 5: Effect of error recovering.

#### 4.3 CASES FROM PROGRESSIVE MODEL

To demonstrate the capability of generating in-the-wild images, we provide our generated results here in Figure 2. Though our base model is much smaller than previous works like Parti, we also achieved a strong performance with a delicate design. Compared with the AR method which gen-





Figure 4: Images from progressive model showing errors in number counting and negative semantic understanding, which motivates future improvements.

erates images from top-left to down-right, our method generates images in a global manner and supports error recovering, resulting in more high-quality and content-rich images. We also list some bad cases in Figure 4 to provide insights on how our approach may be improved. There are representative types of errors, *i.e.*, negative semantic understanding, and spatial relations. Although our approach generates unfavorable images, it still provides related subjects.

## 5 RELATED WORKS

**Autoregressive Image Synthesis.** Currently, autoregressive models (Radford et al., 2018; 2019) have shown promising results for text-to-image generation (Chen et al., 2020; Esser et al., 2021b; Van Den Oord et al., 2017; Parmar et al., 2018; Razavi et al., 2019; Van Oord et al., 2016). Prior works including PixelRNN (Van Oord et al., 2016), Image Transformer (Parmar et al., 2018) and ImageGPT (Chen et al., 2020) factorized the conditional probability on an image over raw pixels. Due to the intolerable amount of computation for large images, modeling images in the low-dimension discrete latent space is introduced. VQ-VAE, VQ-GAN, and ImageBART (Esser et al., 2021a) train an encoder to compress the image and fit the density of the hidden variables. It greatly improves the performance of image generation. More recent DALL-E (Ramesh et al., 2022), CogView (Ding et al., 2021), M6 (Lin et al., 2021), ERINE-ViLG (Zhang et al., 2021), and Parti (Yu et al., 2022b) all use AR-based Transformer architectures in the latent space. In particular, (Lee et al., 2022b) consider global information with refinement by random masking. With a powerful large transformer structure and massive text-image pairs, they greatly advance the quality of text-to-image generation but still ignore the importance and order of image tokens.

**Denosing Diffusion Probabilistic.** Another related work is diffusion generative model, which is first proposed in (Sohl-Dickstein et al., 2015) and achieved strong results on audio (Kong et al., 2020; Jeong et al., 2021), image (Dhariwal & Nichol, 2021; Ho et al., 2020; 2022a; Nichol & Dhariwal, 2021), video (Ho et al., 2022b) generation, and super super-resolution (Saharia et al., 2021). Discrete diffusion models were also first described in (Sohl-Dickstein et al., 2015), and then applied to text generation in ArgmaxFlow (Hoogeboom et al., 2021). D3PMs (Austin et al., 2021) introduce discrete diffusion to image generation. As directly estimating the density of raw image pixels can only generate low-resolution images, more recent works resorts to diffuse in the latent space (Rombach et al., 2022; Gu et al., 2022; Lee et al., 2022c). Generally, our progressive method and diffusion model hold the same process to iterative denoising the image patch, while our method is discretized and has recovering capacity for history error.

## 6 CONCLUSION

This paper argues that the image token is not equal in the latent space and generation order should be considered for text-to-image synthesis. To this end, we introduce a progressive denoising text-to-image generation framework, which powerfully models the image sequence in a coarse-to-fine manner according to the importance score. The resulting top-down hierarchy makes the generation process interpretable and enjoys a significant reduction over empirical time. Experiments show that our progressive model can produce more perceptually compelling samples than conventional autoregressive models. More encouragingly, we look forward to putting forward speed-performance trading and applying the text-to-image model to various practical applications.

---

## REFERENCES

- Peter Anderson, Basura Fernando, Mark Johnson, and Stephen Gould. Spice: Semantic propositional image caption evaluation. In *European conference on computer vision*, pp. 382–398. Springer, 2016.
- Jacob Austin, Daniel D Johnson, Jonathan Ho, Daniel Tarlow, and Rianne van den Berg. Structured denoising diffusion models in discrete state-spaces. *Advances in Neural Information Processing Systems*, 34:17981–17993, 2021.
- Sam Bond-Taylor, Adam Leach, Yang Long, and Chris G Willcocks. Deep generative modelling: A comparative review of vaes, gans, normalizing flows, energy-based and autoregressive models. *IEEE transactions on pattern analysis and machine intelligence*, 2021.
- Tom Brown, Benjamin Mann, Nick Ryder, Melanie Subbiah, Jared D Kaplan, Prafulla Dhariwal, Arvind Neelakantan, Pranav Shyam, Girish Sastry, Amanda Askell, et al. Language models are few-shot learners. *Advances in neural information processing systems*, 33:1877–1901, 2020.
- Soravit Changpinyo, Piyush Sharma, Nan Ding, and Radu Soricut. Conceptual 12m: Pushing web-scale image-text pre-training to recognize long-tail visual concepts. In *Proceedings of the IEEE/CVF Conference on Computer Vision and Pattern Recognition*, pp. 3558–3568, 2021.
- Mark Chen, Alec Radford, Rewon Child, Jeffrey Wu, Heewoo Jun, David Luan, and Ilya Sutskever. Generative pretraining from pixels. In *International conference on machine learning*, pp. 1691–1703. PMLR, 2020.
- Jaemin Cho, Jiasen Lu, Dustin Schwenk, Hannaneh Hajishirzi, and Aniruddha Kembhavi. X-lxmert: Paint, caption and answer questions with multi-modal transformers. In *Proceedings of the 2020 Conference on Empirical Methods in Natural Language Processing (EMNLP)*, pp. 8785–8805, 2020.
- Jaemin Cho, Abhay Zala, and Mohit Bansal. Dall-eval: Probing the reasoning skills and social biases of text-to-image generative transformers. *arXiv preprint arXiv:2202.04053*, 2022.
- Marcella Cornia, Matteo Stefanini, Lorenzo Baraldi, and Rita Cucchiara. Meshed-memory transformer for image captioning. In *Proceedings of the IEEE/CVF conference on computer vision and pattern recognition*, pp. 10578–10587, 2020.
- Michael Denkowski and Alon Lavie. Meteor universal: Language specific translation evaluation for any target language. In *Proceedings of the ninth workshop on statistical machine translation*, pp. 376–380, 2014.
- Prafulla Dhariwal and Alexander Nichol. Diffusion models beat gans on image synthesis. *Advances in Neural Information Processing Systems*, 34:8780–8794, 2021.
- Ming Ding, Zhuoyi Yang, Wenyi Hong, Wendi Zheng, Chang Zhou, Da Yin, Junyang Lin, Xu Zou, Zhou Shao, Hongxia Yang, et al. Cogview: Mastering text-to-image generation via transformers. *Advances in Neural Information Processing Systems*, 34:19822–19835, 2021.
- Ming Ding, Wendi Zheng, Wenyi Hong, and Jie Tang. Cogview2: Faster and better text-to-image generation via hierarchical transformers. *arXiv preprint arXiv:2204.14217*, 2022.
- Xiaoyi Dong, Jianmin Bao, Ting Zhang, Dongdong Chen, Weiming Zhang, Lu Yuan, Dong Chen, Fang Wen, and Nenghai Yu. Peco: Perceptual codebook for bert pre-training of vision transformers. *arXiv preprint arXiv:2111.12710*, 2021.
- Patrick Esser, Robin Rombach, Andreas Blattmann, and Bjorn Ommer. Imagebart: Bidirectional context with multinomial diffusion for autoregressive image synthesis. *Advances in Neural Information Processing Systems*, 34:3518–3532, 2021a.
- Patrick Esser, Robin Rombach, and Bjorn Ommer. Taming transformers for high-resolution image synthesis. In *Proceedings of the IEEE/CVF conference on computer vision and pattern recognition*, pp. 12873–12883, 2021b.

- 
- Oran Gafni, Adam Polyak, Oron Ashual, Shelly Sheynin, Devi Parikh, and Yaniv Taigman. Make-a-scene: Scene-based text-to-image generation with human priors. *arXiv preprint arXiv:2203.13131*, 2022.
- Jiatao Gu and Xiang Kong. Fully non-autoregressive neural machine translation: Tricks of the trade. In *Findings of the Association for Computational Linguistics: ACL-IJCNLP 2021*, pp. 120–133, 2021.
- Jiatao Gu, James Bradbury, Caiming Xiong, Victor OK Li, and Richard Socher. Non-autoregressive neural machine translation. In *International Conference on Learning Representations*, 2018.
- Shuyang Gu, Dong Chen, Jianmin Bao, Fang Wen, Bo Zhang, Dongdong Chen, Lu Yuan, and Baining Guo. Vector quantized diffusion model for text-to-image synthesis. In *Proceedings of the IEEE/CVF Conference on Computer Vision and Pattern Recognition*, pp. 10696–10706, 2022.
- Martin Heusel, Hubert Ramsauer, Thomas Unterthiner, Bernhard Nessler, and Sepp Hochreiter. Gans trained by a two time-scale update rule converge to a local nash equilibrium. *Advances in neural information processing systems*, 30, 2017.
- Jonathan Ho, Ajay Jain, and Pieter Abbeel. Denoising diffusion probabilistic models. *Advances in Neural Information Processing Systems*, 33:6840–6851, 2020.
- Jonathan Ho, Chitwan Saharia, William Chan, David J Fleet, Mohammad Norouzi, and Tim Salimans. Cascaded diffusion models for high fidelity image generation. *J. Mach. Learn. Res.*, 23: 47–1, 2022a.
- Jonathan Ho, Tim Salimans, Alexey A Gritsenko, William Chan, Mohammad Norouzi, and David J Fleet. Video diffusion models. In *ICLR Workshop on Deep Generative Models for Highly Structured Data*, 2022b.
- Emiel Hooeboom, Didrik Nielsen, Priyank Jaini, Patrick Forré, and Max Welling. Argmax flows and multinomial diffusion: Towards non-autoregressive language models. 2021.
- Myeonghun Jeong, Hyeongju Kim, Sung Jun Cheon, Byoung Jin Choi, and Nam Soo Kim. Diff-tts: A denoising diffusion model for text-to-speech. *arXiv preprint arXiv:2104.01409*, 2021.
- Chao Jia, Yinfei Yang, Ye Xia, Yi-Ting Chen, Zarana Parekh, Hieu Pham, Quoc Le, Yun-Hsuan Sung, Zhen Li, and Tom Duerig. Scaling up visual and vision-language representation learning with noisy text supervision. In *International Conference on Machine Learning*, pp. 4904–4916. PMLR, 2021.
- Jeff Johnson, Matthijs Douze, and Hervé Jégou. Billion-scale similarity search with gpus. *IEEE Transactions on Big Data*, 7(3):535–547, 2019.
- Jacob Devlin Ming-Wei Chang Kenton and Lee Kristina Toutanova. Bert: Pre-training of deep bidirectional transformers for language understanding. In *Proceedings of NAACL-HLT*, pp. 4171–4186, 2019.
- Diederik P Kingma and Jimmy Ba. Adam: A method for stochastic optimization. *arXiv preprint arXiv:1412.6980*, 2014.
- Zhifeng Kong, Wei Ping, Jiaji Huang, Kexin Zhao, and Bryan Catanzaro. Diffwave: A versatile diffusion model for audio synthesis. In *International Conference on Learning Representations*, 2020.
- Doyup Lee, Chiheon Kim, Saehoon Kim, Minsu Cho, and Wook-Shin Han. Autoregressive image generation using residual quantization. In *Proceedings of the IEEE/CVF Conference on Computer Vision and Pattern Recognition*, pp. 11523–11532, 2022a.
- Doyup Lee, Chiheon Kim, Saehoon Kim, Minsu Cho, and Wook-Shin Han. Draft-and-revise: Effective image generation with contextual rq-transformer. *arXiv preprint arXiv:2206.04452*, 2022b.
- Sangyun Lee, Hyungjin Chung, Jaehyeon Kim, and Jong Chul Ye. Progressive deblurring of diffusion models for coarse-to-fine image synthesis. *arXiv preprint arXiv:2207.11192*, 2022c.

- 
- Junnan Li, Ramprasaath Selvaraju, Akhilesh Gotmare, Shafiq Joty, Caiming Xiong, and Steven Chu Hong Hoi. Align before fuse: Vision and language representation learning with momentum distillation. *Advances in neural information processing systems*, 34:9694–9705, 2021.
- Junyang Lin, Rui Men, An Yang, Chang Zhou, Ming Ding, Yichang Zhang, Peng Wang, Ang Wang, Le Jiang, Xianyan Jia, et al. M6: A chinese multimodal pretrainer. *arXiv preprint arXiv:2103.00823*, 2021.
- Tsung-Yi Lin, Michael Maire, Serge Belongie, James Hays, Pietro Perona, Deva Ramanan, Piotr Dollár, and C Lawrence Zitnick. Microsoft coco: Common objects in context. In *European conference on computer vision*, pp. 740–755. Springer, 2014.
- Alex Nichol, Prafulla Dhariwal, Aditya Ramesh, Pranav Shyam, Pamela Mishkin, Bob McGrew, Ilya Sutskever, and Mark Chen. Glide: Towards photorealistic image generation and editing with text-guided diffusion models. *arXiv preprint arXiv:2112.10741*, 2021.
- Alexander Quinn Nichol and Prafulla Dhariwal. Improved denoising diffusion probabilistic models. In *International Conference on Machine Learning*, pp. 8162–8171. PMLR, 2021.
- Kishore Papineni, Salim Roukos, Todd Ward, and Wei-Jing Zhu. Bleu: a method for automatic evaluation of machine translation. In *Proceedings of the 40th annual meeting of the Association for Computational Linguistics*, pp. 311–318, 2002.
- Niki Parmar, Ashish Vaswani, Jakob Uszkoreit, Lukasz Kaiser, Noam Shazeer, Alexander Ku, and Dustin Tran. Image transformer. In *International conference on machine learning*, pp. 4055–4064. PMLR, 2018.
- Alec Radford, Karthik Narasimhan, Tim Salimans, Ilya Sutskever, et al. Improving language understanding by generative pre-training. 2018.
- Alec Radford, Jeffrey Wu, Rewon Child, David Luan, Dario Amodei, Ilya Sutskever, et al. Language models are unsupervised multitask learners. *OpenAI blog*, 1(8):9, 2019.
- Alec Radford, Jong Wook Kim, Chris Hallacy, Aditya Ramesh, Gabriel Goh, Sandhini Agarwal, Girish Sastry, Amanda Askell, Pamela Mishkin, Jack Clark, et al. Learning transferable visual models from natural language supervision. In *International Conference on Machine Learning*, pp. 8748–8763. PMLR, 2021.
- Colin Raffel, Noam Shazeer, Adam Roberts, Katherine Lee, Sharan Narang, Michael Matena, Yanqi Zhou, Wei Li, Peter J Liu, et al. Exploring the limits of transfer learning with a unified text-to-text transformer. *J. Mach. Learn. Res.*, 21(140):1–67, 2020.
- Aditya Ramesh, Mikhail Pavlov, Gabriel Goh, Scott Gray, Chelsea Voss, Alec Radford, Mark Chen, and Ilya Sutskever. Zero-shot text-to-image generation. In *International Conference on Machine Learning*, pp. 8821–8831. PMLR, 2021.
- Aditya Ramesh, Prafulla Dhariwal, Alex Nichol, Casey Chu, and Mark Chen. Hierarchical text-conditional image generation with clip latents. *arXiv preprint arXiv:2204.06125*, 2022.
- Ali Razavi, Aaron Van den Oord, and Oriol Vinyals. Generating diverse high-fidelity images with vq-vae-2. *Advances in neural information processing systems*, 32, 2019.
- Robin Rombach, Andreas Blattmann, Dominik Lorenz, Patrick Esser, and Bjorn Ommer. High-resolution image synthesis with latent diffusion models. In *Proceedings of the IEEE/CVF Conference on Computer Vision and Pattern Recognition*, pp. 10684–10695, 2022.
- Chitwan Saharia, Jonathan Ho, William Chan, Tim Salimans, David J Fleet, and Mohammad Norouzi. Image super-resolution via iterative refinement. *arXiv preprint arXiv:2104.07636*, 2021.
- Chitwan Saharia, William Chan, Saurabh Saxena, Lala Li, Jay Whang, Emily Denton, Seyed Kamyar Seyed Ghasemipour, Burcu Karagol Ayan, S Sara Mahdavi, Rapha Gontijo Lopes, et al. Photorealistic text-to-image diffusion models with deep language understanding. *arXiv preprint arXiv:2205.11487*, 2022.



- 
- Jascha Sohl-Dickstein, Eric Weiss, Niru Maheswaranathan, and Surya Ganguli. Deep unsupervised learning using nonequilibrium thermodynamics. In *International Conference on Machine Learning*, pp. 2256–2265. PMLR, 2015.
- Richard S Sutton, David McAllester, Satinder Singh, and Yishay Mansour. Policy gradient methods for reinforcement learning with function approximation. *Advances in neural information processing systems*, 12, 1999.
- Christian Szegedy, Vincent Vanhoucke, Sergey Ioffe, Jon Shlens, and Zbigniew Wojna. Rethinking the inception architecture for computer vision. In *Proceedings of the IEEE conference on computer vision and pattern recognition*, pp. 2818–2826, 2016.
- Bowen Tan, Zichao Yang, Maruan Al-Shedivat, Eric Xing, and Zhiting Hu. Progressive generation of long text with pretrained language models. In *Proceedings of the 2021 Conference of the North American Chapter of the Association for Computational Linguistics: Human Language Technologies*, pp. 4313–4324, 2021.
- Aaron Van Den Oord, Oriol Vinyals, et al. Neural discrete representation learning. *Advances in neural information processing systems*, 30, 2017.
- Aaron Van Oord, Nal Kalchbrenner, and Koray Kavukcuoglu. Pixel recurrent neural networks. In *International conference on machine learning*, pp. 1747–1756. PMLR, 2016.
- Ashish Vaswani, Noam Shazeer, Niki Parmar, Jakob Uszkoreit, Llion Jones, Aidan N Gomez, Łukasz Kaiser, and Illia Polosukhin. Attention is all you need. *Advances in neural information processing systems*, 30, 2017.
- Ramakrishna Vedantam, C Lawrence Zitnick, and Devi Parikh. Cider: Consensus-based image description evaluation. In *Proceedings of the IEEE conference on computer vision and pattern recognition*, pp. 4566–4575, 2015.
- Chenfei Wu, Jian Liang, Xiaowei Hu, Zhe Gan, Jianfeng Wang, Lijuan Wang, Zicheng Liu, Yuejian Fang, and Nan Duan. Nuwa-infinity: Autoregressive over autoregressive generation for infinite visual synthesis. *arXiv preprint arXiv:2207.09814*, 2022.
- Jiahui Yu, Xin Li, Jing Yu Koh, Han Zhang, Ruoming Pang, James Qin, Alexander Ku, Yuanzhong Xu, Jason Baldridge, and Yonghui Wu. Vector-quantized image modeling with improved vqgan. *arXiv preprint arXiv:2110.04627*, 2021.
- Jiahui Yu, Zirui Wang, Vijay Vasudevan, Legg Yeung, Mojtaba Seyedhosseini, and Yonghui Wu. Coca: Contrastive captioners are image-text foundation models. *arXiv preprint arXiv:2205.01917*, 2022a.
- Jiahui Yu, Yuanzhong Xu, Jing Yu Koh, Thang Luong, Gunjan Baid, Zirui Wang, Vijay Vasudevan, Alexander Ku, Yinfei Yang, Burcu Karagol Ayan, et al. Scaling autoregressive models for content-rich text-to-image generation. *arXiv preprint arXiv:2206.10789*, 2022b.
- Han Zhang, Weichong Yin, Yewei Fang, Lanxin Li, Boqiang Duan, Zhihua Wu, Yu Sun, Hao Tian, Hua Wu, and Haifeng Wang. Ernie-vilg: Unified generative pre-training for bidirectional vision-language generation. *arXiv preprint arXiv:2112.15283*, 2021.

---

## A EXPERIMENTAL SETTINGS

**Datasets for Training and Evaluation.** We train on a combination of image-text datasets for progressive model training, including a filtered subset of LAION-400M and Conceptual Captions-3M. For all image inputs, we follow the VQ-GAN (Esser et al., 2021b) input processing with weight trained on ImageNet to pre-extract the image token sequence. To demonstrate the capability of our proposed method for text-to-image synthesis, we conduct experiments on the MS COCO dataset (Lin et al., 2014), which currently is a standard benchmark for text-to-image performance evaluation. MS COCO dataset contains 82k images for training and 40k images for testing. Each image in this dataset has five human-annotated text descriptions.

**Implementation Details.** For the image tokenizer, we follow the setting of original VQ-GAN (Esser et al., 2021b), which leverages the GAN loss to get a more realistic image. The codebook size is 163,84 with dimension 256, and the compression ratio 16. That is, it converts  $512 \times 512$  images into  $32 \times 32$  tokens. We directly adopt the publicly available VQ-GAN model trained on the ImageNet dataset for all text-to-image synthesis experiments<sup>1</sup>. We adopt a publicly available tokenizer of the base version of t5 (Raffel et al., 2020) as a text encoder. For the decoder of the text-to-image transformer, we set the stacked layer number to 24, the hidden dimension to 1280, the feed-forward dimension to 4096, and the head number to 20. An additional linear layer is appended at the last transformer layer to predict the state sequence. For error recovering, we select  $p_{error} = 0.4$  by default. Both image and text encoders in our training are frozen. We use AdamW (Kingma & Ba, 2014) optimizer with  $\beta_1 = 0.9$  and  $\beta_2 = 0.96$ . The model is trained for 120 epochs with the cosine learning rate schedule with the initial value of  $1e-4$ .

## B HUMAN EVALUATION

We follow (Yu et al., 2022b) to conduct side-by-side human evaluations, in which human annotators are presented with two outputs for the same prompt and are asked to choose which image is a higher quality and more natural image (image realism) and which is a better match to the input prompt (image-text alignment). As for the Turing test, the model types are anonymized and randomly shuffled for each presentation to an annotator, and each pair is judged by three independent annotators.

	Image Realism			Image-Text Match		
	baseline wins	border	prog. wins	baseline wins	border	prog. wins
minDALL-E	34.3	24.2	41.5	33.0	31.2	35.8
Random	31.2	29.7	39.2	33.7	27.8	38.5

Table 6: Human evaluation results over 200 randomly sampled prompts and the corresponding generated images from the MS COCO test set.

The results are summarized and shown in Table 6. We require the annotators from two perspectives: image realism and image-text match. As we can see, our progressive model significantly outperforms minDALL-E, which is the popular open-source autoregressive image generation model and holds a similar model parameter and training data size. On the other hand, when compared against the random mode with the same network architecture, our progressive model still shows superiority for optimized generation order.

---

<sup>1</sup><https://github.com/CompVis/taming-transformers>